OUKA
The University of Osaka
Institutional Knowledge Archive

Title	Antibacterial Cu-doped calcium phosphate coating on pure titanium
Author(s)	Li, Qiang; Yang, Jinshuai; Li, Junjie et al.
Citation	Materials Transactions. 2021, 62(7), p. 1052-1055
Version Type	VoR
URL	https://hdl.handle.net/11094/89891
rights	
Note	

The University of Osaka Institutional Knowledge Archive : OUKA

https://ir.library.osaka-u.ac.jp/

The University of Osaka

Materials Transactions, Vol. 62, No. 7 (2021) pp. 1052 to 1055
©2021 The Japan Institute of Metals and Materials
EXPRESS RAPID PUBLICATION

Antibacterial Cu-Doped Calcium Phosphate Coating on Pure Titanium

Qiang Li[1,*], Jinshuai Yang[1], Junjie Li[2], Ran Zhang[1], Masaaki Nakai[3], Mitsuo Niinomi[1,4,5,6,7,*] and Takayoshi Nakano[5]

[1]*School of Mechanical Engineering, University of Shanghai for Science and Technology, Shanghai 200093, P. R. China*
[2]*CAS Key Laboratory of Functional Materials and Devices for Special Environments, Xinjiang Technical Institute of Physics & Chemistry, CAS; Xinjiang Key Laboratory of Electronic Information Materials and Devices, 40-1 South Beijing road, Urumqi 830011, P. R. China*
[3]*Department of Mechanical Engineering, Faculty of Science and Engineering, Kindai University, Higashiosaka 577-8502, Japan*
[4]*Institute for Materials Research, Tohoku University, Sendai 980-5377, Japan*
[5]*Division of Materials and Manufacturing Science, Graduate School of Engineering, Osaka University, Suita 565-0871, Japan*
[6]*Department of Materials Science and Engineering, Graduate School of Science and Technology, Meijo University, Nagoya 468-8502, Japan*
[7]*Faculty of Chemistry, Materials and Bioengineering, Kansai University, Osaka 564-860, Japan*

Cu-doped amorphous calcium phosphate (ACP) coatings were fabricated on the surface of pure titanium (Ti) by electrochemical deposition at initial electrolyte temperatures of 35, 45, and 55°C. The antibacterial activities of the coatings were then evaluated by the plate counting method using *Escherichia coli* as the indicator. The Cu concentrations on the surfaces of samples are increased from 6.90 to 15.05 mass% as initial electrolyte temperature is increased from 35 to 55°C. The Cu-doped ACP coatings show that they can fully inhibit the growth of *E. coli*.
[doi:10.2320/matertrans.MT-M2021005]

(Received January 18, 2021; Accepted April 14, 2021; Published June 25, 2021)

Keywords: *biomaterials, hydroxyapatite, antibacterial coating, electrochemical deposition*

1. Introduction

Pure titanium (Ti) and Ti alloys are widely used as biomedical implant materials, and an increasing number of studies have focused on preparing calcium phosphate coatings on the surfaces of Ti implants. Many studies indicate that calcium phosphate coatings have good osseointegration and biocompatibility, which enables the implant to integrate well with natural bone.[1)] Some metallic ions are doped in calcium phosphate coatings to allow better coating functionality. Sr^{2+} can promote the synthesis of new osteoblasts by promoting the production of collagen and alkaline phosphatase, and inhibit bone resorption by reducing osteoclast activity.[2)] Mg^{2+} can regulate bone mineralization and promote bone growth and remodeling.[3)] Ag, Zn, and Cu-doped hydroxyapatites show antibacterial effects, which can reduce the possibility of implant loosening or implant failures caused by bacterial infections.[4)] However, Ag^{+} is expensive and shows high cytotoxicity. Meanwhile, Cu^{2+} shows the best antibacterial effect compared with Zn^{2+} and Ag^{+} and shows low cytotoxicity.[5)] Many studies focus on Cu-doped hydroxyapatite (HA) coatings rather than Cu-doped amorphous calcium phosphate (ACP) coatings.

Although HA is the main inorganic component of human hard tissue, the amorphous nature of ACP is very important for the realization of specific physiological functions.[6)] Compared with HA, ACP particles can also destroy the stability of bacterial cell membrane and inhibit the growth of bacteria.[7)]

In this study, Cu-doped antibacterial amorphous coatings were electrochemically deposited on Ti substrates via Cu-containing Ca–P solutions at different initial temperatures. The Cu content, morphologies, and antibacterial properties of the coatings were also evaluated.

2. Materials and Methods

Ti plates (99.9% purity; hereafter, % means mass%) with dimensions 10 mm × 10 mm × 1 mm were polished using 120–5000 grade sandpaper. Then, calcium phosphate coatings were prepared by a double electrode system using Ti as the cathode and Pt as the anode. The electrolyte consisted of 0.025 M $NH_4H_2PO_4$ and 0.042 M $CaCl_2{\cdot}2H_2O$, and was maintained in a 45°C water bath during the entire deposition process. To dope the coating with Cu, 10% of the Ca^{2+} were replaced by Cu^{2+} in the electrolyte. Thus, the electrolyte for the Cu-doped coating consisted of 0.025 M $NH_4H_2PO_4$, 0.0378 M $CaCl_2{\cdot}2H_2O$, and 0.0042 M $CuCl_2{\cdot}2H_2O$. During deposition of the Cu-doped coatings, the water bath temperatures were set to three values, namely 35, 45, and 55°C. All the electrochemical depositions were performed at a voltage of 3.2 V and deposition time of 30 min. Thereafter, the samples were cleaned with deionized water and dried at ambient temperature.

The surface morphologies of the samples were observed by scanning electron microscope (SEM) and energy dispersive spectroscopy (EDS) to characterize the elemental composition. The coating phases were detected by X-ray diffraction (XRD), and the chemical state of Cu in the coating was analyzed by AIXS Ultra DLD X-ray photoelectron spectroscopy (XPS) with monochromatic Al Kα ($h\nu$ = 1486.6 eV) X-ray as the radiation source. The sample was pasted on the sample table, put into the instrument, and then tested under vacuum. Electron flood gun was used for charge compensation. The binding energy scale was calibrated from the hydrocarbon contamination using the C 1s peak at 248.8 eV.

*Corresponding authors, E-mail: jxli@tju.edu.cn & liqiang@usst.edu.cn; niinomi@imr.tohoku.ac.jp

The antibacterial properties of the coatings were evaluated by the plate counting method using *E. coli* (ATCC25922) as indicator. Before the test, all samples were sterilized at 121°C for 30 min by autoclave. The concentration of *E. coli* suspension was adjusted to 10^9 CFU/L by using sterilized muller-hinton (MH) liquid medium, and 2×10^{-4} L of the suspension was dripped on the surface of each sample. The samples with suspension were incubated at 37°C for 18 h, and then eluted by 1.8×10^{-3} L sterile phosphate buffer solution (PBS) to remove the bacteria solution on the surface. The eluent was finally diluted 10^4 times by serial dilution. 10^{-4} L of the diluted eluent was spread evenly on a MH medium agar plate and then put in a thermostat at 37°C for 18 h. After that, the visible cells of each plate were counted by quantifying the CFU. Each test was performed in triplicate.

The Cu-doped ACP with the lowest Cu content was subjected to Cu ion release test. It was placed in a bottle contained 0.02 L PBS at 37°C for 24 h, and then the concentration of Cu^{2+} in the solution was tested by inductively coupled plasma mass spectrometer (ICP-MS).

3. Results and Discussion

3.1 XRD results

Figure 1 shows the XRD patterns of the coatings prepared at different electrolyte temperatures. The diffraction peaks of α-Ti at 35.0°, 38.3° and 40.1° are detected in all samples. A typical diffraction peak of HA at 21.7°, 22.8° and 26.0° is observed in Fig. 1(a), indicating that the calcium phosphate coating mainly comprises HA. No obvious peaks corresponding to calcium phosphates are detected by XRD in the Cu-doped coatings, and a broad peak was seen at approximately 30° (Fig. 1(b), 1(c), and 1(d)), indicating that the coating mainly comprises ACP.[8] The Cu diffraction peaks are found at 43.3° in Fig. 1(b), 1(c), and 1(d).

When the Ca^{2+} is replaced by other metal ions, the apatite crystallinity is reduced, and nucleation and growth of the apatite crystals are inhibited.[9] In this study, the appearance of ACP is attributed to the inhibition of HA crystal growth by Cu^{2+}.

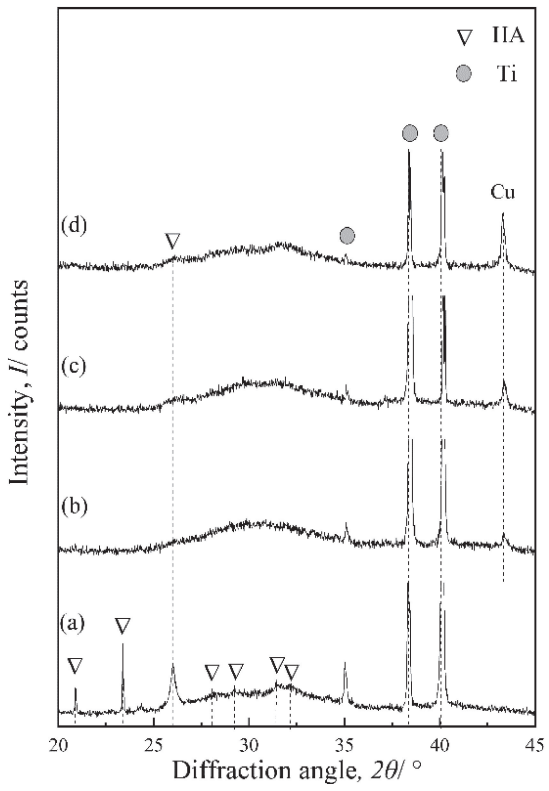

Fig. 1 XRD patterns of calcium phosphate coatings prepared at different electrolyte temperatures: (a) pure calcium phosphate coating prepared at 45°C; Cu-doped calcium phosphate coatings prepared at (b) 35, (c) 45, and (d) 55°C.

3.2 Characterization

Figure 2 shows the SEM images of the surfaces of the coatings. The calcium phosphate coating without Cu shows dense and uniform needle-like structures on the surface (Fig. 2(a)). When Cu^{2+} ions are added and the electrolyte is maintained at 45°C, flocculent white particles appear on the surface (Fig. 2(c)). As temperature is decreased to 35°C, only primary spherical particles are seen on the substrate (Fig. 2(b)). When the temperature is increased to 55°C, the substrate is completely covered by the dense flocculent particles (Fig. 2(d)). Cu mapping shows that Cu is uniformly deposited on the coating surface. The thickness of the coating is increased from 0.56 to 1.10 μm with the increase of deposition temperature (Fig. 3).

Table 1 lists the main chemical compositions of the samples measured by EDS. The proportions of Cu and Ca in the samples are increased with increasing temperatures, but the Ti content is decreased. The deposition of calcium phosphate is controlled by charge transfer kinetics, and the deposition speed is improved by increasing the temperature.[10,11] The Ti surface is more extensively covered by the calcium phosphate coating at higher temperatures; thus, Ti content is decreased with increasing Cu and Ca contents at higher temperatures. By removing the Ti content, the percentages of Cu content in the coatings deposited at

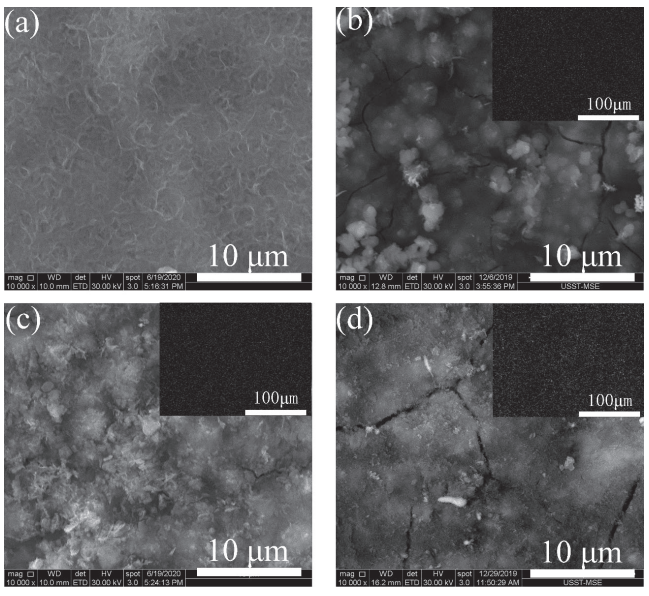

Fig. 2 SEM images and Cu mapping images of different calcium phosphate coatings: (a) pure calcium phosphate coating; Cu-doped calcium phosphate prepared at (b) 35, (c) 45, and (d) 55°C.

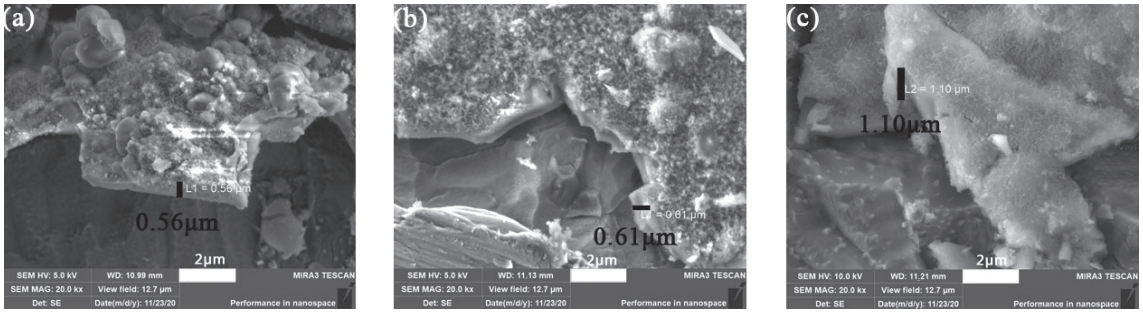

Fig. 3 SEM images for the thickness of the Cu-doped calcium phosphate coatings prepared at (a) 35, (b) 45, and (c) 55°C.

Table 1 Main elemental compositions of the sample surfaces after calcium phosphate coating at different electrolyte temperatures.

Temperature (°C)	Main elements (mass. %)				(Cu+Ca)/P molar ratio	Corresponding SEM images
	Cu	Ca	P	Ti		
45	0	9.41	10.98	64.26	0.66	Fig. 2(a)
35	6.90	14.65	16.16	60.81	0.91	Fig. 2(b)
45	9.24	15.99	15.55	55.63	1.09	Fig. 2(c)
55	15.05	18.78	15.38	35.08	1.42	Fig. 2(d)

temperatures of 35, 45, and 55°C are recalculated to 17.61%, 20.82% and 23.18%, respectively. Additionally, the Ca/P molar ratio are increased, because more PO_4^{3-} ions are produced with increasing electrolyte temperatures,[11] and HPO_4^{3-} is replaced in ACP.[12] In this study, Cu^{2+} ions are used to partly replace Ca^{2+}; thus, the (Ca + Cu)/P molar ratio is also increased with temperature. Moreover, Cu^{2+} is more easily bound to PO_4^{3-} and OH^- than Ca^{2+}. Therefore, the Cu content in the coating is evidently increased. When the doping amount of Cu^{2+} in HA reaches saturation,[13] Cu^{2+} can directly obtain electrons at the cathode to generate Cu through a reduction reaction. This explains why a Cu diffraction peak is detected in the XRD pattern. With the increase of deposition temperature, the peek intensity of Cu becomes stronger indicating an increase of the metallic Cu content.

3.3 XPS results

Figure 4 shows the Cu $2p_{3/2}$ spectrums and Cu LMM auger spectrums of the coatings. There are strong satellite peaks in the range 940–950 eV, indicating the existing of Cu^{2+} in the coatings.[14–16] The peaks of Cu (II) $2p_{3/2}$ spectrum are located at approximately 934.6 eV and 936.3 eV, which can be assigned to $Cu(OH)_2$ and $CuHPO_4$.[14,17] The peak located at about 932.9 eV attributed to the presence of Cu (0) or Cu (I).[14,16] Because of their similar binding energies, it is difficult to identify the chemical state of Cu only by analyzing Cu $2p_{3/2}$ spectrums. Auger electron spectroscopy has been generally used to further confirm it. The peak of Cu LMM Auger spectrum located at about 918.5 eV is very close to that of Cu metal,[14] indicating that Cu metal exists in the coating. This is consistent with the result in XRD.

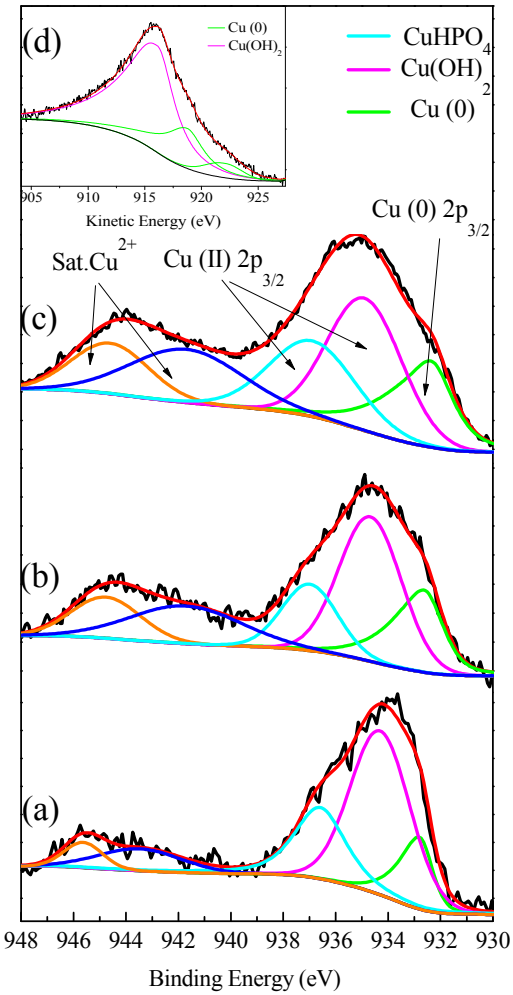

Fig. 4 Cu $2p_{3/2}$ XPS core peak of Cu-doped calcium phosphate coatings prepared at (a) 35, (b) 45, (c) 55°C, and (d) Cu LMM Auger spectrum of the coating prepared at 55°C.

3.4 Antibacterial activity

The apatite coating without Cu does not show antibacterial

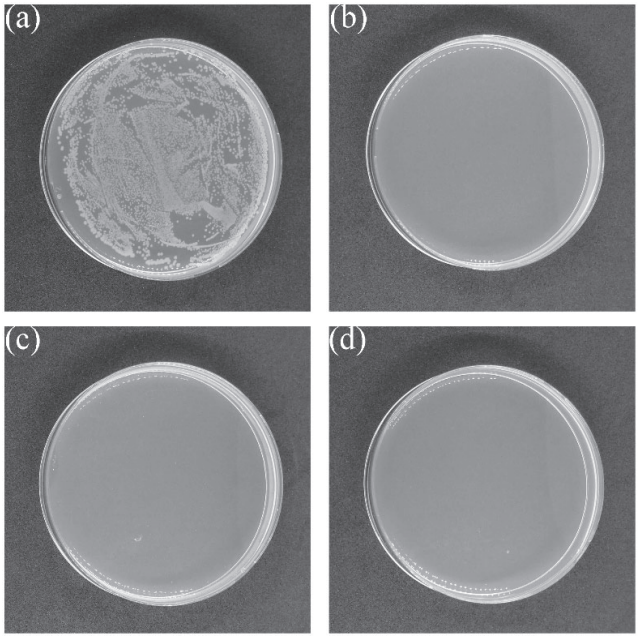

Fig. 5 Antibacterial activities of calcium phosphate coatings against *E. coli*: (a) pure calcium phosphate coating; Cu-doped calcium phosphate coatings prepared at (b) 35, (c) 45, and (d) 55°C.

Table 2 *E. coli* colony counts on the sample surfaces after calcium phosphate coating at different electrolyte temperatures by antibacterial tests.

Sample	Cu content (mass. %)	*E. coli* colony counts (CFU)
Pure apatite (35°C)	0	$6.63 \pm 0.57 \times 10^3$
Cu-ACP (35°C)	6.90	0
Cu-ACP (45°C)	9.24	0
Cu-ACP (55°C)	15.05	0

effects. A large number of *E. coli* colonies can be observed in the agar plate (Fig. 5(a)), and the *E. coli* number is $6.63 \pm 0.57 \times 10^3$ CFU (Table 2). However, such *E. coli* colonies are not observed in Fig. 5(b), 5(c), and 5(d), and the *E. coli* number is 0 (Table 2), indicating that the antimicrobial ratio is higher than 99%. According to the XPS results, the main compounds in the coating are $Cu(OH)_2$ and $CuHPO_4$, which have low solubility. The results show that the quantity of Cu^{2+} release is 0.157 mg/L, which is higher than that of the HA coatings prepared by D. Sivaraj *et al.* (0.042 mg/L),[7] but lower than that of the HA powders prepared by S. Gomes *et al.* (at least 0.4 mg/L).[15] It has been reported that Cu^{2+} can destroy the cell wall of *E. coli*, enter the cell membrane, inhibit the transport and metabolism of sugar, lead to the destruction of metal ion homeostasis and enzyme system, and finally kill *E. coli*.[18] The prepared Cu-doped coatings, having higher Cu content, show better antibacterial effects than previously reported Cu-HA coatings with low Cu content of 0.80%, which have an antimicrobial ratio of only >75%.[4] S. Gomes *et al.* also point out that favored proliferation for cells is still maintained although the release of Cu^{2+} reaches 0.4 mg/L.[15] Thus, the currently used electrochemical deposition parameters can be applied to prepare antibacterial coatings on Ti implants.

4. Conclusion

Cu-doped amorphous calcium phosphate coatings were electrochemically deposited on Ti surfaces using an electrolyte consisting of $NH_4H_2PO_4$, $CaCl_2 \cdot 2H_2O$, and $CuCl_2 \cdot 2H_2O$. The Cu content in the coatings was increased from 6.90 to 15.05% as the electrolyte temperatures were increased from 35 to 55°C. The Cu-doped coatings are shown to completely inhibit the growth of *E. coli*, thereby proving their excellent antibacterial properties. The proposed electrochemical deposition method is thus feasible for improving the antibacterial behaviors of coated implants.

Acknowledgement

This work was partially supported by the Natural Science Foundation of Shanghai, China (No. 15ZR1428400), National Natural Science Foundation of China (No. 51771120 and 51304136), the project of Creation of Life Innovation Materials for Interdisciplinary and International Researcher Development, Tohoku University, Japan sponsored by Ministry, Education, Culture, Sports, Science and Technology, Japan, and the Grant-in-Aid for Scientific Research (C) (No. 20K05139) from JSPS (Japan Society for the Promotion of Science), Tokyo, Japan.

REFERENCES

1) E. Boanini, M. Gazzano and A. Bigi: Acta Biomater. **6** (2010) 1882–1894.
2) E. Boanini, P. Torricelli, F. Sima, E. Axente, M. Fini, I.N. Mihailescu and A. Bigi: J. Colloid Interface Sci. **448** (2015) 1–7.
3) M. Kawashita, S. Itoh, K. Miyamoto and G.H. Takaoka: J. Mater. Sci. Mater. Med. **19** (2008) 137–142.
4) Y. Huang, X. Zhang, R. Zhao, H. Mao, Y. Yan and X. Pang: J. Mater. Sci. **50** (2015) 1688–1700.
5) E. Zhang, F. Li, H. Wang, J. Liu, C. Wang, M. Li and K. Yang: Mater. Sci. Eng. C **33** (2013) 4280–4287.
6) R. Gelli, F. Ridi and P. Baglioni: Adv. Colloid Interface Sci. **269** (2019) 219–235.
7) D. Sivaraj, K. Vijayalakshmi, A. Ganeshkumar and R. Rajaram: Int. J. Pharm. **590** (2020) 119946.
8) K. Rubenis, S. Zemjane, J. Vecstaudza, J. Bitenieks and J. Locs: J. Eur. Ceram. Soc. **41** (2021) 912–919.
9) K.A. Gross, L. Komarovska and A. Viksna: J. Aust. Ceram. Soc. **49** (2013) 129–135.
10) C.M. Cotrut, A. Vladescu, M. Dinu and D.M. Vranceanu: Ceram. Int. **44** (2018) 669–677.
11) N. Eliaz: Isr. J. Chem. **48** (2008) 159–168.
12) C. Combes and C. Rey: Acta Biomater. **6** (2010) 3362–3378.
13) M.G. Martínez, D.P. Minh, E. Weiss-Hortala, A. Nzihou and P. Sharrock: Compos. Interfaces **20** (2013) 647–660.
14) M.C. Biesinger: Surf. Interface Anal. **49** (2017) 1325–1334.
15) S. Gomes, C. Vichery, S. Descamps, H. Martinez, A. Kaur, A. Jacobs, J.M. Nedelec and G. Renaudin: Acta Biomater. **65** (2018) 462–474.
16) X. Zhang, X. Huang, Y. Ma, N. Lin, A. Fan and B. Tang: Appl. Surf. Sci. **258** (2012) 10058–10063.
17) X. Lu, Z. Huang, Z. Liang, Z. Lie, J. Yang, Y. Wang and F. Wang: Sci. Total Environ. **764** (2021) 144269.
18) D. Sivaraj, K. Vijayalakshmi, A. Ganeshkumar and R. Rajaram: Int. J. Pharm. **590** (2020) 119946.